Journal of
Medicinal Chemistry

Article

A novel decalin-based bicyclic scaffold for FKBP51-selective ligands

Xixi Feng, Claudia Sippel, Fabian Knaup, Andreas Bracher,
Stefania Staibano, Maria Fiammetta Romano, and Felix Hausch

J. Med. Chem., **Just Accepted Manuscript** • DOI: 10.1021/acs.jmedchem.9b01157 • Publication Date (Web): 04 Dec 2019

A novel decalin-based bicyclic scaffold for FKBP51-selective ligands

Xixi Feng[†,‡], Claudia Sippel[†,§], Fabian Knaup[⁎], Andreas Bracher[#], Stefania Staibano[∥], Maria F. Romano[‡], Felix Hausch[⁎,]*

[†] Max Planck Institute of Psychiatry, Dept. Translational Research in Psychiatry, Kraepelinstrasse 2, 80804 Munich, Germany

[#] Max Planck Institute of Biochemistry, Am Klopferspitz 18, 82152 Martinsried, Germany

[‡]Department of Molecular Medicine and Medical Biotechnologies, Federico II University, 80131 Naples, Italy

[∥]Department of Advanced Biomedical Sciences, Federico II University of Naples, 80131 Naples, Italy

[⁎] Institute for Organic Chemistry and Biochemistry, Technische Universität Darmstadt, Alarich-Weiss-Strasse 4, D-64287 Darmstadt, Germany

Present address:

‡ Merck Holding (China) Co., 201203, Shanghai, P.R.China

§Pieris Pharmaceuticals GmbH, 85354, Freising, Germany

*Correspondence: hausch@drugdiscovery.chemie.tu-darmstadt.de; Tel.: +49-6151-16-21245

KEYWORDS: FKBP51, decalin, FK506, immunophilins, isomerase,

ABSTRACT

Selective inhibition of FKBP51 has emerged as possible novel treatment for diseases like major depressive disorder, obesity, chronic pain and certain cancers. The current FKBP51 inhibitors are rather large, flexible and have to be further optimized. Using a structure-based rigidification strategy, we hereby report the design and synthesis of a novel promising bicyclic scaffold for FKBP51 ligands. The structure-activity analysis revealed the decalin scaffold as the best moiety for the selectivity-enabling subpocket of FBKP51. The resulting compounds retain high potency for FKBP51 and excellent selectivity over the close homolog FKBP52. With the cocrystal structure of an advanced ligand in this novel series, we show how the decalin locks the key selectivity-inducing cyclohexyl moiety of the ligand in a conformation typical for FKBP51-selective binding. The best compound **29** produces cell death in a HeLa-derived KB cell line, a cellular model of cervical adenocarcinoma, where FKBP51 is highly overexpressed. Our results show how FKBP51

inhibitors can be rigidified and extended while preserving FKBP51 selectivity. Such inhibitors might be novel tools in the treatment of human cancers with deregulated FKBP51.

INTRODUCTION

The FK506-binding protein 51 (FKBP51, encoded by the FKBP5 gene) belongs to the immunophilin family and acts as a cochaperone in the Hsp90 machinery[1, 2]. It functions in part by regulating glucocorticoid receptor and NFκB signaling.[3-4] Human genetic studies have repeatedly associated FKBP51 with stress-related mental disorders such as depression.[5,6] FKBP51 knockout mice displayed antidepressant-like behavior[7-9], had an improved stress hormone regulation[7-9], sleep pattern[10], and glucose tolerance[11,12], and were protected from weight gain after a high fat die[11,12] and several forms of chronic pain[13,14]. Moreover, FKBP51 is highly overexpressed in certain cancer types such as gliomas or melanomas where it seems to promote cancer progression or resistance to chemo-or irradiation therapy via modulating NFκB or PD-L1 signaling.[4,15]

A key problem in FKBP51 drug discovery is to achieve selectivity over its close homolog FKBP52. Due to the high structural homology between these proteins, prototypical ligands derived from FK506 exhibit similar binding affinities to both proteins. Concomitant binding, however, has to be avoided since both proteins have opposing effects, e.g. in neuronal cells.[25] An inhibition of FKBP52 is even predicted to have toxic effects since a knockout of this protein in mice led to severe impairment of the reproduction system.[26,27]

We recently discovered a transient binding pocket in FKBP51, which is highly disfavored for FKBP52 due to different dynamics in the two proteins. SAFit1 and SAFit2, the most advanced FKBP51 inhibitors so far, stabilize this transient pocket and are highly selective for FKBP51 over

FKBP52 (Fig. 1). In mice, SAFit2 had antidepressant-like effects[29,32], attenuated weight gain[11], pain hypersensitivity[13,14] and inappropriate alcohol consumption[33], and facilitated glucose uptake in human primary adipocytes.[34] Most recently, we showed that FKBP51 inhibition can attenuate tumor progression in a mouse model of glioblastoma.[15]

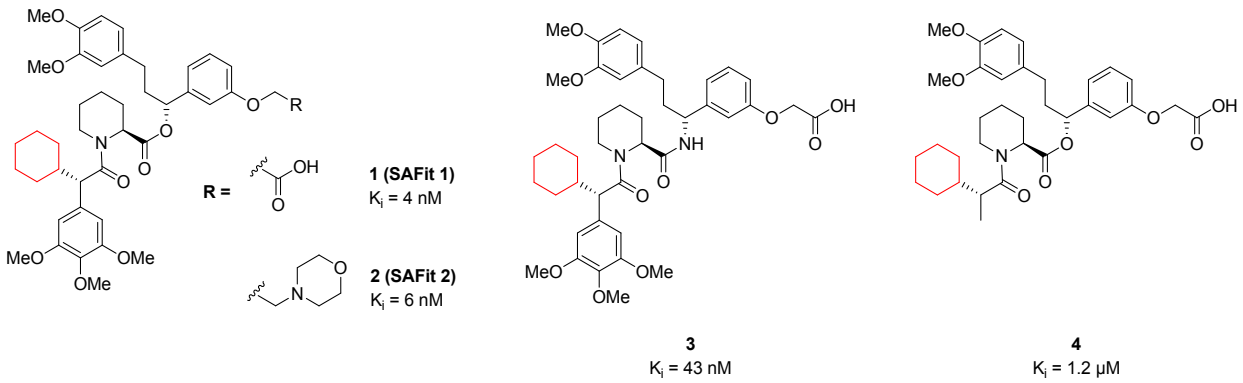

Figure 1: Chemical structures of the FKBP51-selective ligands SAFit1 (**1**), SAFit2 (**2**), the SAFit1 analog **3**, analog **4,** and their binding affinities towards FKBP51. The cyclohexyl moiety, which imparts selectivity for FKBP51 over FKBP52, is highlighted in red.

However, SAFit1 and SAFit2 are unsuitable as drug candidates and the development of improved analogs has been challenging. Initial structure-activity relationship analyses revealed that the SAFit scaffold generally has poor ligand efficiency. SAFit1 and SAFit2 are highly flexible molecules that possess >12 rotatable bonds. The aim of this study was to explore rigidified SAFit analogs as improved starting points for the development of FKBP51-selective compounds.

Results and Discussion

Rigidification for improving binding affinity

During the discovery of SAFit2, the cyclohexyl ring was found to be the most critical structural feature for high selectivity against FKBP52.[29] Replacing it with smaller substituents led to a significant loss of both selectivity and binding affinity. In contrast, the trimethoxyphenyl ring was shown to be important for high binding affinity but not for selectivity *per se*. Replacing it by different aliphatic substituents and alcohols retained an FKBP51-preferring, induced fit-like binding mode. A simple methyl group as in compound **4** (Fig. 1) was identified as the minimal selectivity-inducing moiety.[30]

In order to improve the affinity of the FKBP51-selective ligands, we set out to explore a preorganization strategy. A closer inspection of the available cocrystal structures of SAFit analogs in complex with FKBP51 revealed that the trimethoxyphenyl ring as well as the cyclohexyl ring are positioned in a way that suggested a possible cyclization by an ethylene linker (Fig. 2, compare with crystal structure in Fig. 4)[35].

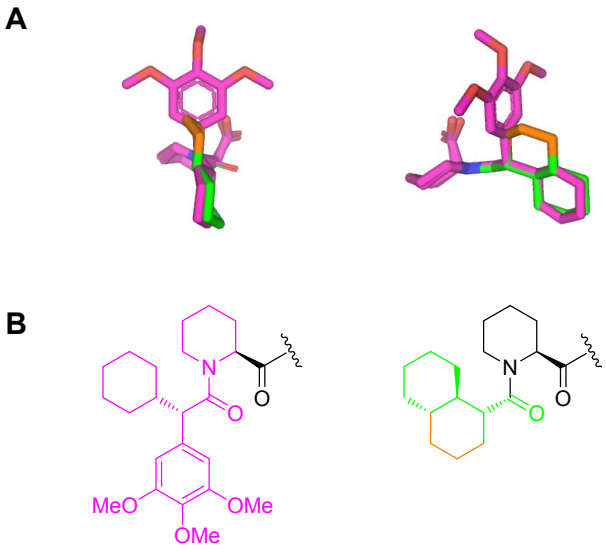

Figure 2: A rigidification strategy to increase binding affinity. (A) The bottom part of the SAFit1-analog compound **3** from Gaali et al.[31] is shown as sticks (magenta) in its active conformation

bound to FKBP51 (pipecolic amide substituent is not shown for clarity). The decalin-derived scaffold is superimposed (green sticks). The ethylene linker is highlighted in orange. (B) The chemical structures of the respective stick representations.

We first started with a screening of ligands that contained a bicyclic aromatic moiety instead of the trimethoxyphenyl-cyclohexyl group of SAFit1 (Fig. 3). All compounds were synthesized by solid phase-assisted synthesis[19], using commercially available aromatic carboxylic acids. Unfortunately, no binding towards FKBP51 was observed in a fluorescence polarization assay[36] up to the solubility limits of the compounds (>10μM in all cases). For analogs harboring an aromatic or unsaturated carbon in the Cα-position such as **5a-e** or **5g**, this can be explained by the need to break conjugation with the adjacent carbonyl group as well as an unfavorable fit of the planar geometry of the aromatic bicycles, which may not fit to the shape of the FKBP51 binding pocket (Suppl. Fig. S5). However, compound **5f** can be modelled to adopt a conformation that closely mimics the binding mode of SAFit-like ligands (Fig. 3B). These findings suggest that the selectivity-inducing subpocket in FKBP51 is very sensitive to the precise geometry of the interacting moieties.

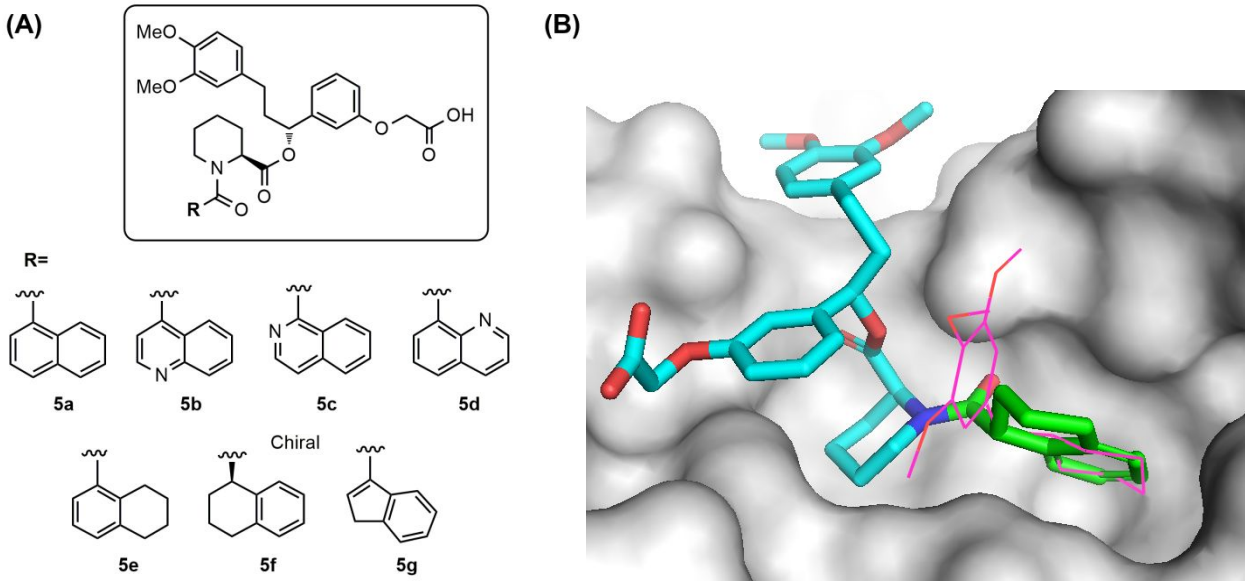

Figure 3: (A) Chemical structures of synthetic ligands that contain an aromatic bicycle instead of the trimethoxyphenyl-cyclohexyl group of SAFit1. (B) Compound **5f** modelled in the binding site of FKBP51 (PDB-ID: 5DIU). Compound **3** is shown superimposed as magenta lines. Lys^{121} has been removed for clarity.

We therefore set out to synthesize exactly the saturated, stereochemically defined bicyclic structure derived from our modelling studies. Although this decalin structure is substantially more complex, all three stereocenters can be conceptually generated in a single step by an intramolecular Diels-Alder cyclization.

Synthesis of a novel bicyclic FKBP51 ligand series

The key step of the decalin synthesis is a dimethylaluminium chloride-promoted (DMAC) cyclization of trienimides **10a-c**, whereby the stereochemistry is directed by an Evans auxiliary (Scheme 1). To obtain the trienimides for cyclization we developed a synthesis that is significantly shorter than original synthetic procedure reported by Evans[37] (3 steps instead of 6 to synthesize the methyltrienoates **8a-c**). In addition, our synthesis is more adjustable for the introduction of substituents.

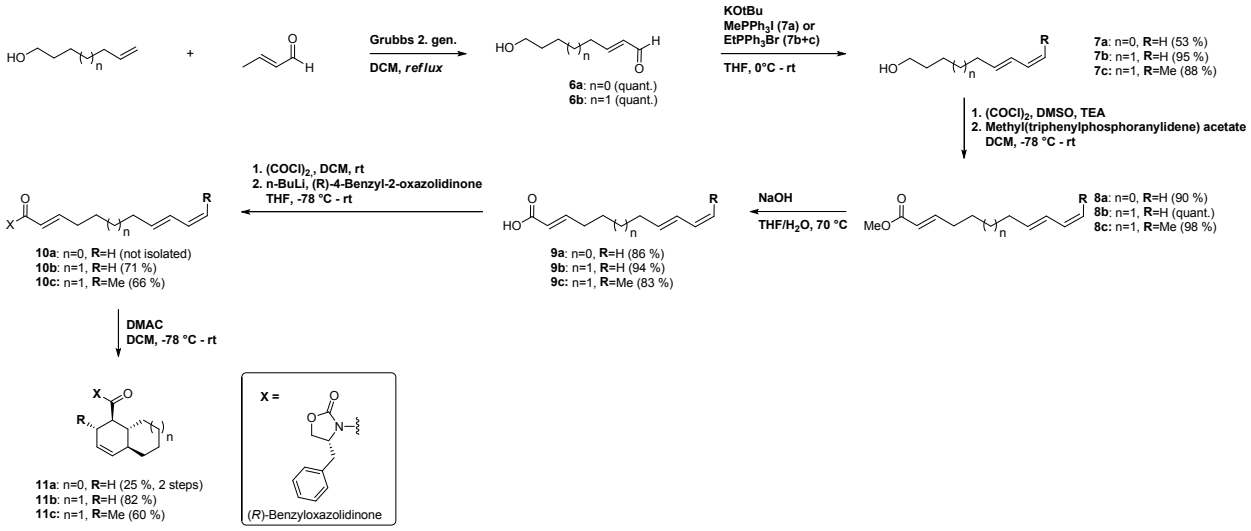

Scheme 1: Reagents and conditions used for the synthesis of **11 a-c**. The obtained yields are stated in parentheses.

The synthesis of the triene-chain starts with a cross metathesis between an alkenol and trans-crotonaldehyde[38] to exclusively yield the (*E*)-products **6a** and **6b**. In the following step the α,β-unsaturated aldehydes are converted by a Wittig reaction to the dienols **7a-c**. The dienol **7c** was obtained in an E/Z ratio of 1:4. Due to the wide range of commercially available Wittig reagents, it is possible to introduce different moieties in this step that will result in a substituent in 2-position

of the cyclized decalins. To further extend the chain at the opposite end the alcohols **7a-c** were first converted under Swern conditions to aldehydes and elonged by adding Methyl(triphenylphosphoranylidene) acetate directly to the reaction mixture. This step mainly provided the *E*-isomers **8a-c**. The small amounts of the formed *Z*-isomers (~ 5 %) can easily be separated from the desired trienoate by flash chromatography. To obtain the free carboxylic acids **9a-c** the methyl esters were cleaved in a mixture of 2 M aqueous NaOH and THF respectively. The Evans auxiliary was introduced to the trienoic acids by acetylation with the respective acid chlorides of **9a-c** or directly with a coupling reagent. The following DMAC-promoted cyclizations of the trienimides proceeded smoothly, yielding the desired *trans*–cycloadducts as single diastereomers **11a-c**.

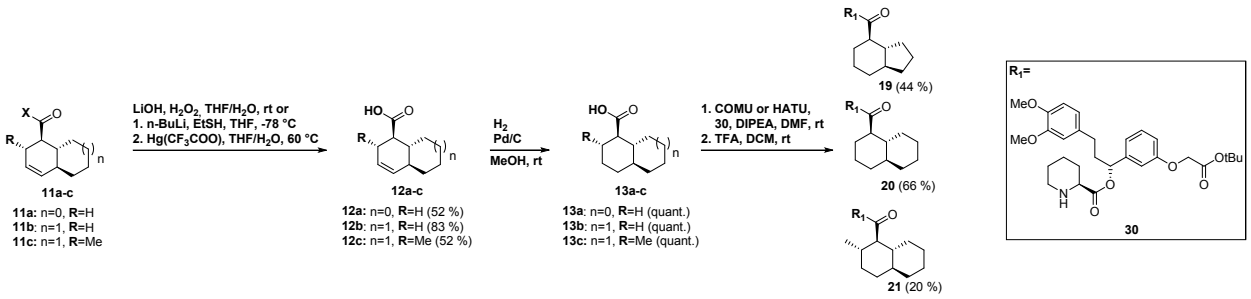

Scheme 2: Synthesis of the intermediates **12a-c** and their conversion in to their SAFit 1 analogues.

To explore the aliphatic bicyclic substituents in more detail, the decalin and bicyclo[4.3.0]nonan scaffolds were further derivatized. After cyclization, the chiral auxiliary (Scheme 2) of the unsubstituted bicycles **11a** and **11b** was cleaved with LiOOH to obtain the free carboxylic acids **12a** and **12b** respectively. Bicycle **11c**, which is substituted in the 2-position, was first converted to the respective thioester and then hydrolyzed with mercury (II) trifluoroacetate to yield **12c**[39]. Hydrogenation catalyzed by Pd/C provided the respective saturated bicycles **13a-c**.

The free carboxylic acids were coupled to **30** or **31** with 1-[Bis(dimethylamino)methylene]-1H-1,2,3-triazolo[4,5-b]pyridinium 3-oxid hexafluorophosphate (HATU) or (1-Cyano-2-ethoxy-2-oxoethylidenaminooxy)dimethylamino-morpholino-carbenium hexafluorophosphate (COMU) as coupling reagent to obtain the final compounds as SAFit1 (after tBu deprotection) or SAFit2 derivatives respectively.

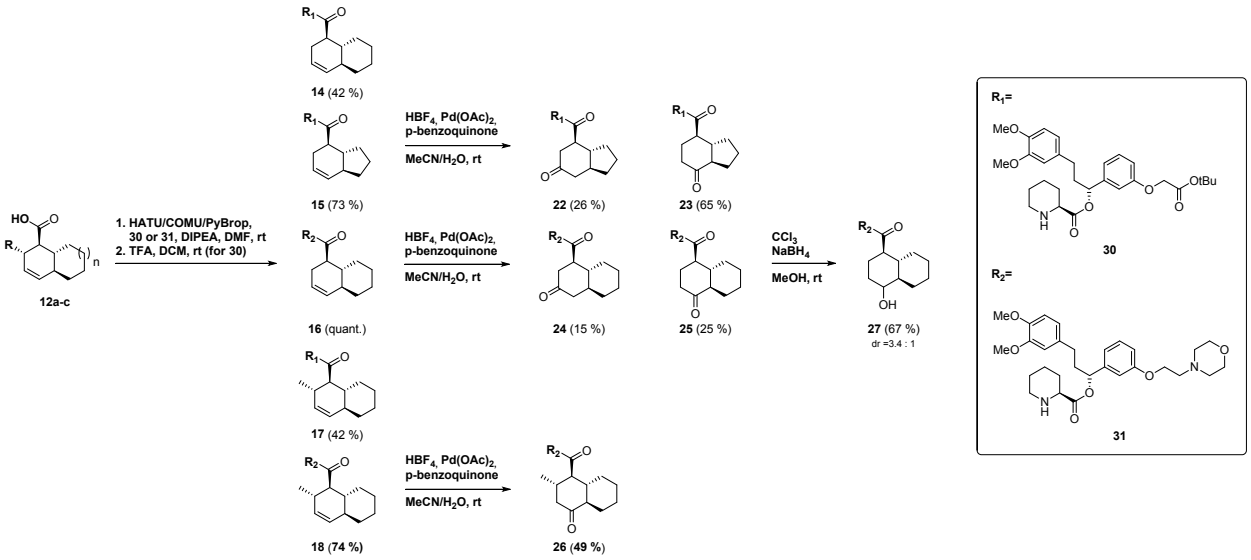

Scheme 3: Synthesis of the SAFit analogues **14-18** and further derivatization of those, via Wacker conditions and Luche reduction (**22-27**).

15 and **16** were oxidized under Wacker conditions[40] to obtain the 3-keto (**22, 24**) and the 4-keto (**23, 25**) compounds in a 1:2.5 ratio, which can be easily separated by flash chromatography. In contrast, oxidation of **18** only provided the respective 4-keto compound **26**. The carbonyl group of **25** was further reduced via Luche reduction[41] to yield **27** in a diasteromeric ratio of 3.4:1.

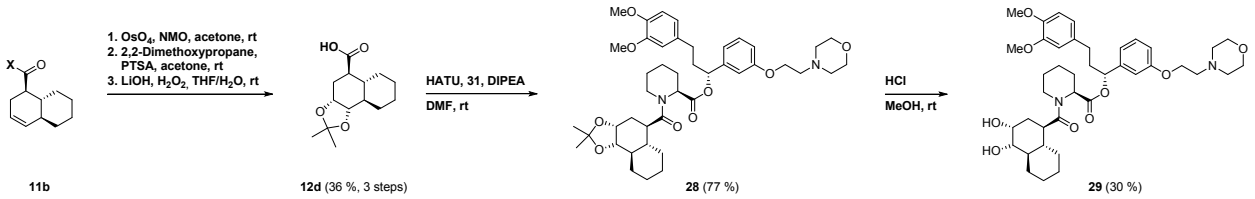

Scheme 4: Synthesis of the protected dihydroxylated analogue **28** and its dihydroxy compound **29**.

To obtain **12d**, a dihydroxylation step was conducted with OsO_4 and **11b**. After protection of the diol, the minor diastereomer was removed by flash chromatography. Then the auxiliary was cleaved and the free carboxylic acid was coupled to **31** to obtain **28.** The dihydroxy compound **29** was obtained after treatment of **28** under acidic conditions.

Structure-Affinity Relationship (SAR) of the new FKBP51-selective ligand series

Compounds **14-29** were tested in a competitive fluorescence polarization assay for binding to FKBP51 and FKBP52. All bicycles showed binding towards FKBP51 but almost no binding towards FKBP52 was observed. This is in agreement with our modelling studies that one of the bicyclic rings corresponds to the cyclohexyl substituent that was previously reported to be important for FKBP51 selective ligands.

In general, we observed that the [4.3.0] bicycles, containing octahydro-indene and derivatives, show lower binding affinities towards FKBP51 than their corresponding decalin-compounds. Additionally, all decalin-like compounds showed no binding towards FKBP52, whereas one octahydro-indene derivative (**23**) showed low binding towards FKBP52. In all cases, a saturation of the double bond, a leftover of the intramolecular Diels-Alder cyclization, resulted in a significant increase in binding affinity (compare **14/20, 15/19, 17/21**). The addition of a methyl

group in the 2-position of the decalins was tolerated (**26/25**, **18/16**) or led to a slight increase in affinity (**21** vs **20**).

We next explored the appendage of polar groups in the ring systems. Carbonyl groups in the 3-position had negative effects on the binding affinity (**22** vs **19**, **24** vs **20**)[42]. However, a carbonyl group in the 4-position improved affinity (**25** vs **20**, **26** vs **21**), resulting in a K_i= 0.23 μM for **25**. A hydroxyl group in the 4-position was less effective (**27** vs **25**). The dihydroxylated derivative **29** showed improved binding (K_i = 0.28 μM), suggesting beneficial interactions of the 3-hydroxy group. The free hydroxyl groups seemed to be important since alkylation of the hydroxy groups as in **28** significantly decreases the binding affinity.

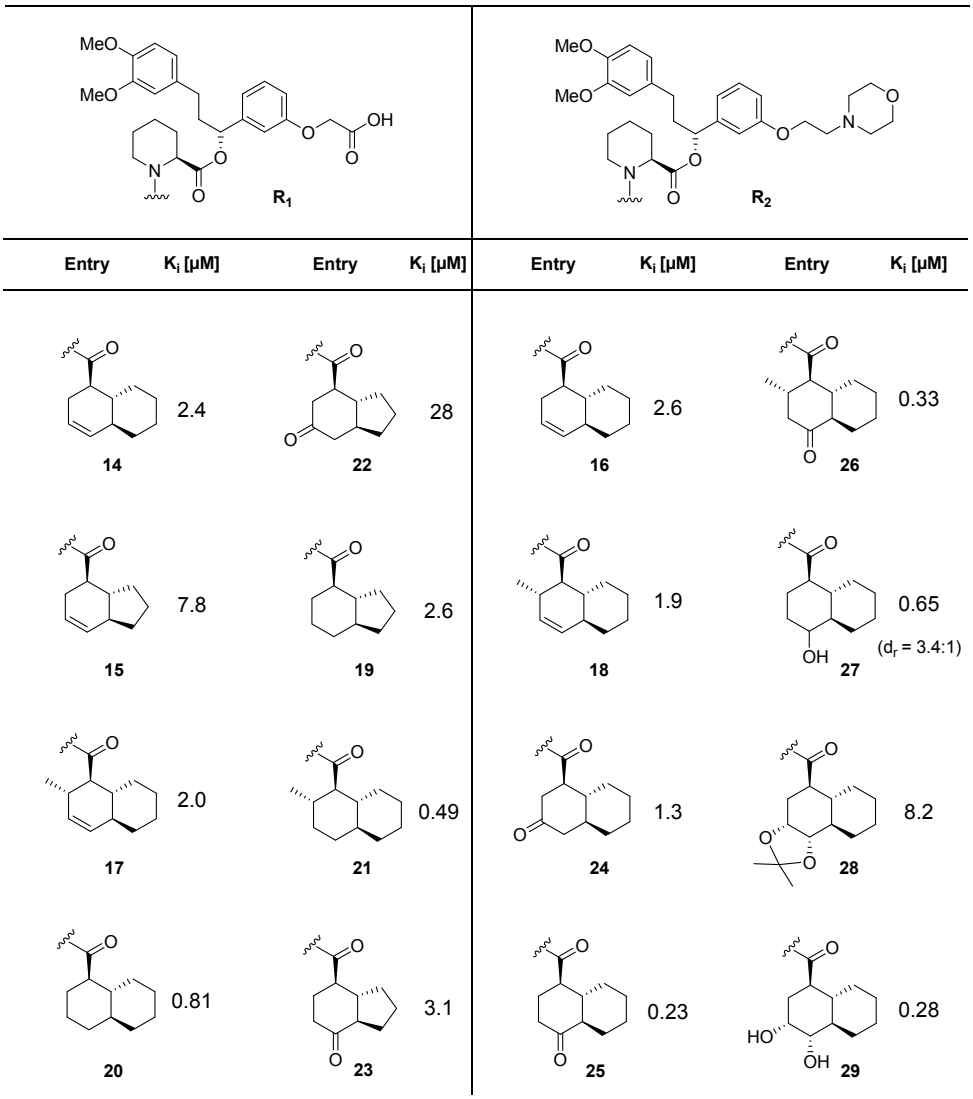

Table 1. FKBP binding affinities bicyclic SAFit1 (**1**) and SAFit2 (**2**) analogs; Ki values were determined by a competitive fluorescence polarization assay[36]; **25** was tested as diastereomeric mixture (3.4:1).

In an exploratory assessment of the drug-like parameter of the currently most advanced FKBP51 SAFit1 and SAFit2, inhibition of CYP3A4 was identified as an inacceptable liability (IC_{50} for SAFit2 <1μM). Gratifyingly, compound **20** showed reduced CYP3A4 inhibition (estimated IC_{50}

= 8.4µM, Suppl. Fig. S6) suggesting that the rigidified analogs of the decalin series could provide compounds with an improved ADME/PK profile (Suppl. Table 2).

*Cocrystal structure of **25***

To confirm the postulated binding mode of our decalin-containing analogs, we solved a cocrystal structure of **25** in complex with the FK506-binding domain of FKBP51 (Fig. 4)[43]. The X-ray structure revealed a binding conformation that is in agreement with previously described FKBP ligands. The pipecolic ester is centered in a hydrophobic pocket. The prominent hydrogen bonds to Ile87 and Tyr113, which until now have been observed in all FKBP51 complexes with carbonyl pipecolate-based ligands are also present (Fig. 4A). We were delighted to see that that the conformational rearrangement of Phe67, which is indicative for FKBP51-selective binding, is preserved. The terminal cyclohexyl ring of the decalin is deeply buried in the enlarged binding pocket created by the conformational rearrangement of Phe67, and it superimposes almost perfectly with cyclohexyl substituent of cocrystallized ligands of the SAFit series (Fig. 4B). Close contacts of the 4-keto group of **25** with Lys121 of FKBP51 were observed.

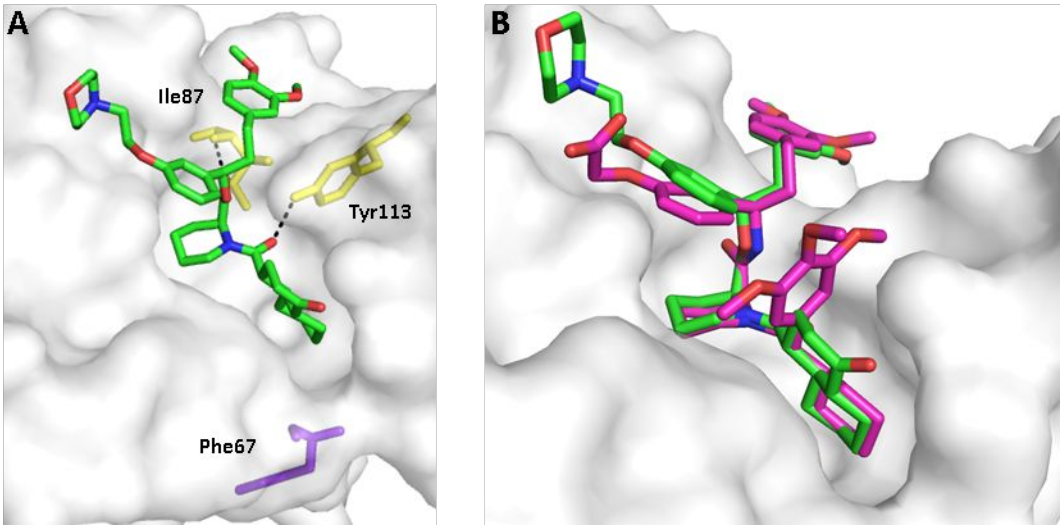

Figure 4: X-ray structures of **25** (green) in complex with the FK506-binding domain of FKBP51 (grey surface); Lys121 has been omitted for clarity. (A) Hydrogen bonds to Tyr113 (yellow) and Ile87 (yellow) are indicated as black dotted lines. The displaced Phe67 is shown as purple sticks. (B) The SAFit1 analog 3 (magenta, from 5DIU)) has been superimposed on the **25**-FKBP51 complex

*Pro-apoptotic effects of **29***

Because FKBP51 sustains cancer resistance, we evaluated the anti-cancer effect of the advanced compound **29** using the HeLa-derived KB cell line as a model system, based on the finding that, in this cell line, FKBP51 transcript is at least ten-fold higher compared with mRNA level of two different melanoma cell lines (Suppl. Fig. 1). Cells were cultured at different doses with the compound and cell death was determined after 72h. As shown in Fig. 5a, the cytotoxic effect of the compound increased in a dose-dependent manner. To address whether cells died by apoptosis, cells, stimulated with **29** were harvested after 40h and stained with annexin V and PI. The proportion of died cells with an intact membrane (annexin V+/PI-), consistent with early apoptosis,

was measured. Fig. 5b shows the proportion of annexin V+/PI- progressively increased in the presence of **29** in a dose-dependent manner, suggesting the cells died by apoptosis and confirming the anti-cancer effect **29**. The FKBP51 inhibitors SAFit1 and SAFit2 similarly induced apoptosis in KB cells at 1µM, in line with their enhanced affinity to FKBP51 (see Suppl. Fig. 2 for a full dose-response relationship for SAFit1 and SAFit2). The apoptotic effect of compound **29** as well as of SAFit2 were higher in KB cells (expressing high levels of FKBP51) compared with the progenitor HeLa cells (expressing low levels of FKBP51, Suppl. Fig. 3). This suggests an addiction of KB cells to FKBP51, which in turn leads to a higher sensitivity to FKBP51 inhibitors. To further confirm the specificity of **29**, we tested the close analog **5a**, which does not bind to FKBP51, in KB cells. As expected, **5a** did not induce cell death up to a concentration of 60µM (Suppl. Fig. S4). Collectively, these data strongly suggest FKBP51 as a relevant target for the apoptotic activities of **29**.

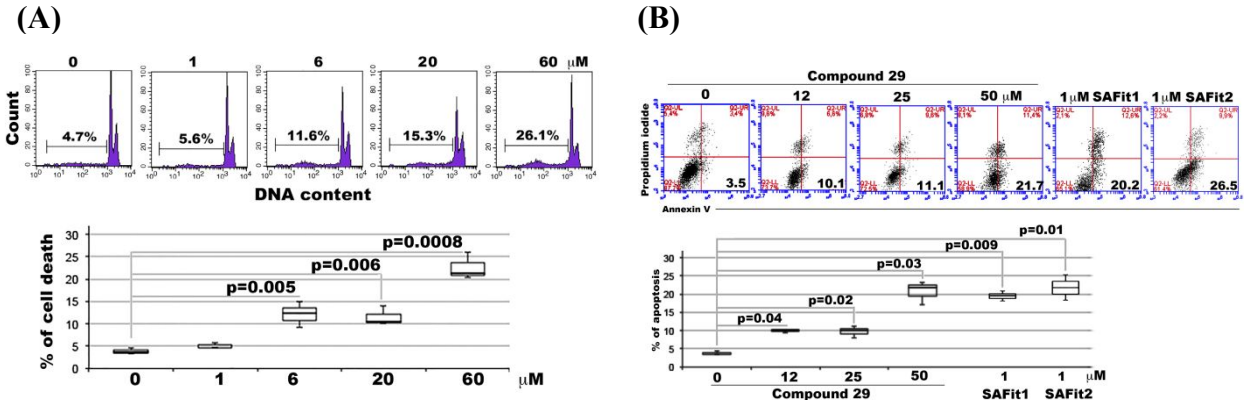

Figure 5: Compound **29** dose-dependently enhances cell death of KB cells. (A) Cells were incubated with compound **29** at different doses. Cell death was measured after 72h by PI incorporation and measurement of hypodiploid cells. Representative histograms of KB cell DNA content are shown on top. Boxplots below represent values of hypodiploid (dead) cells from four experiments, each performed in triplicate. (b) Cells were incubated with **29** at different doses and with SAFit 1 and 2, which were used as positive control for FKBP51 inhibition. Cell death was

measured after 40h by annexin V/PI double staining to determine apoptosis. Representative histograms of KB cell apoptosis are shown on top. Boxplots represent values of annexinV+/PI- cells (corresponding to early apoptosis) from four experiments each performed in triplicate.

Conclusion

In order to explore the binding of selective FKBP51 antagonists, we used a rigidification strategy to design a novel scaffold for new FKBP51 ligands. The resulting decalin analogs bound with exactly the same binding mode as noncyclic cyclohexyl derivatives. The direct comparison of the underivatized decalin analog **20** with the methyl-containing compound **4** (Fig. 1) shows that the cyclization *per se* only minimally enhances binding affinity. However, the constrained decalin scaffold provides several new rigid exit vectors, which are not possible for the parent cyclohexyl-containing SAFit analogs. This can be exploited to further enhance affinity, as shown for compounds **25** and **29**. These analogs are rapidly accessible using the improved synthesis developed for the decalin scaffold. Using these analogs, we show that selective FKBP51 inhibitors impair the viability of cancer cells. Collectively, our findings substantially improve our understanding of FKBP51 inhibitors and provide a new rigidified scaffold for future optimization of FKBP51-directed drugs.

Experimental Section:

All dry reactions were performed under argon atmosphere and with commercially available dry solvents. Chromatographic separations were performed either by manual flash chromatography or automated flash chromatography using an Interchim Puriflash 430 with an UV detector. Merck F-254 (thickness 0.25 mm) commercial plates were used for analytical TLC. ^{1}H NMR spectra, ^{13}C

NMR spectra, 2D HSQC, HMBC, and COSY of all intermediates were obtained from the Department of Chemistry and Pharmacy, Ludwig-Maximilians-University Munich, on a Bruker Avance III HD 400/800 or a Varian NMR system 300/400/600 at room temperature. Chemical shifts for 1H or 13C are given in ppm (δ) downfield from tetramethylsilane using residual protio solvent as an internal standard. Mass spectra (m/z) were recorded on a Thermo Finnigan LCQ DECA XP Plus mass spectrometer at the Max Planck Institute of Psychiatry, while the high resolution mass spectrometry was carried out at MPI for Biochemistry (Microchemistry Core Facility) on Bruker Daltonics MicrOTOF. Purities of all tested compounds were greater than 95% based on HPLC chromatograms. HPLC analyses were performed on a Beckman System Gold 125S Solvent Module fitted with a Phenomenex Jupiter 4µm Proteo 90Å column (250 mm x 4.6 mm) and a Beckman System Gold Diode Array Detector Module 168 (220 nm). The following buffers were used: buffer A: 0.1% TFA in H_2O and buffer B: 0.1% TFA in MeCN. Unless otherwise indicated, in the supporting information, samples were run at a gradient of 0 - 100% B over 20 min at a flow rate of 1.5 mL/min.

(E)-8-hydroxyoct-2-enal (6b). To a solution of Grubbs 2nd generation catalyst (85.0 mg, 100 µmol) in 50 mL DCM was added hept-6-en-1-ol (1.35 mL, 10.0 mmol) and crotonaldehyde (4.14 mL, 50.0 mmol). The reaction mixture was heated to reflux for 2 h (oil bath was preheated to 50 °C). After completion of the reaction the mixture was cooled to rt. Some silica gel was added to the flask and the resulting slurry was stirred open to air for 30 min. The solvent was removed and the crude product was purified by flash chromatography (0-40 % EtOAc in cyclohexane) to obtain the title compound as light brown oil (quantitative yield). ^{1}H NMR (599 MHz, $CDCl_3$) δ 9.49 (d, J = 7.9 Hz, 1H), 6.83 (dt, J = 15.6, 6.8 Hz, 1H), 6.10 (ddt, J = 15.6, 7.9, 1.5 Hz, 1H), 3.64 (t, J = 6.5 Hz, 2H), 2.38 – 2.30 (m, 2H), 1.61 – 1.56 (m, 2H), 1.55 – 1.50 (m, 2H), 1.44 – 1.38 (m, 2H).^{13}C

NMR (151 MHz, $CDCl_3$) δ 194.07, 158.54, 133.04, 62.63, 32.63, 32.36, 27.61, 25.32. MS (ESI^+): calc. 165.09 $[C_8H_{14}O_2+Na]^+$, found 164.08 $[M+Na]^+$.

(E)-nona-6,8-dien-1-ol (7b). To a suspension of ethyltriphenylphosphonium bromide (6.68 g, 18 mmol) in 90 mL THF, KOtBu (19.5 mL, 19.50 mmol, 1 M in THF) was added dropwise at 0 °C. The solution was stirred at rt for 1 h and then again cooled to 0 °C. The aldehyde **6b** (1.07 g, 7.50 mmol) dissolved in 8 mL THF was then added dropwise and the mixture was stirred at 4 °C for 16 h. After warming to rt the reaction was quenched by the addition of a saturated NH_4Cl solution and the product was extracted several times with Et_2O. The combined organic layers were dried over $MgSO_4$, filtered and the solvent was removed under reduced pressure. The crude product was purified by flash chromatography (0-40 % EtOAc in cyclohexane) as a yellow oil (1.0g, 7.14 mmol, 95.1 %).

^1H NMR (300 MHz, $CDCl_3$) δ 6.31 (dt, J = 16.9, 10.2 Hz, 1H), 6.12 – 5.99 (m, 1H), 5.70 (dt, J = 14.6, 6.9 Hz, 1H), 5.14 – 5.04 (m, 1H), 4.99 – 4.92 (m, 1H), 3.64 (t, J = 6.6 Hz, 2H), 2.18 – 2.00 (m, 2H), 1.68 – 1.49 (m, 2H), 1.47 – 1.32 (m, 5H). ^{13}C NMR (75 MHz, $CDCl_3$) δ 137.23, 135.12, 131.07, 114.73, 62.92, 32.61, 32.44, 28.94, 25.29. MS (ESI^+): calc. 141.23 $[C_9H_{16}O+H]^+$, found 140.90 $[M+H]^+$.

(2E,8E)-methyl undeca-2,8,10-trienoate (8b). DMSO (1.06 mL, 14.97 mmol) was added to a solution of oxalyl chloride (3.74 mL, 7.49 mmol, 2 M in DCM) in 50 mL DCM at -78 °C and stirred at that temperature for 30 min. Then the alcohol **7b** (700 mg, 4.99 mmol), dissolved in 5 mL DCM was added and the reaction mixture was stirred for further 60 min at -78 °C. In the following step TEA (6.96 mL, 49.90 mmol) was added and the slurry was allowed to warm to rt.

Then methyl 2-(triphenylphosphoranylidene)acetate (1.84 g, 5.49 mmol) was added in one portion and the slurry was stirred at rt for additional 16 h. The reaction mixture was then washed with H_2O and saturated NH_4Cl solution. The organic layer was then dried over $MgSO_4$, filtered and the solvent was removed under reduced pressure. The product **8b** was obtained after purification by flash chromatography (0-5 % EtOAc in cyclohexane) as a yellow oil (quantitative yield). ^{1}H NMR (400 MHz, $CDCl_3$) δ 6.95 (dt, *J* = 15.7, 7.0 Hz, 1H), 6.42 – 6.19 (m, 1H), 6.13 – 5.97 (m, 1H), 5.81 (dt, *J* = 15.6, 1.6 Hz, 1H), 5.75 – 5.58 (m, 1H), 5.15 – 5.03 (m, 1H), 5.03 – 4.86 (m, 1H), 3.72 (s, 3H), 2.20 (qd, *J* = 7.0, 1.6 Hz, 2H), 2.12 – 2.01 (m, 2H), 1.52 – 1.36 (m, 4H). ^{13}C NMR (101 MHz, $CDCl_3$) δ 167.11, 149.41, 137.13, 134.71, 131.25, 120.97, 114.92, 51.37, 32.20, 32.00, 28.57, 27.48, 26.89. MS (ESI^+), calc. 195.14 $[C_{12}H_{18}O_2+H]^+$, found 195.01 $[M+H]^+$.

(2E, 8E)- undeca-2,8,10-trienoic acid (9b). The methyl ester **8b** (680 mg, 3.50 mmol) was dissolved in 35 mL THF/2 M aq. NaOH (1.5:1) and stirred at 70 °C until the reaction was finished. After cooling to rt the reaction mixture was extracted with Et_2O. The organic layer was removed and the aqueous layer acidified with concentrated HCl. Then free carboxylic acid was extracted several times with DCM. The combined organic layers were dried over $MgSO_4$, filtered and the solvent was removed under reduced pressure to obtain the product **9b** as a light yellow oil (595 mg, 3.30 mmol, 94.3 %) without further purification.

^{1}H NMR (400 MHz, $CDCl_3$) δ 7.07 (dt, *J* = 15.6, 7.0 Hz, 1H), 6.30 (dtd, *J* = 17.0, 10.2, 0.7 Hz, 1H), 6.21 – 5.92 (m, 1H), 5.82 (dt, *J* = 15.6, 1.6 Hz, 1H), 5.78 – 5.55 (m, 1H), 5.15 – 5.05 (m, 1H), 5.05 – 4.85 (m, 1H), 2.23 (qd, *J* = 6.9, 1.6 Hz, 2H), 2.18 – 2.03 (m, 2H), 1.62 – 1.30 (m, 4H).^{13}C

NMR (101 MHz, $CDCl_3$) δ 171.79, 152.04, 137.11, 134.63, 131.30, 120.71, 114.96, 32.19, 32.11, 28.59, 27.34. MS (ESI^+), calc. 181.12 $[C_{11}H_{16}O_2+H]^+$, found 181.00 $[M+H]^+$.

(*R*)-4-benzyl-3-((2E,8E)-undeca-2,8,10-trienoyl)oxazolidin-2-one (10b). The carboxylic acid **9b** (900 mg, 4.99 mmol) was dissolved in 5 mL DCM and oxalyl chloride (4.99 mL, 9.98 mmol, 2 M in DCM) with a catalytic amount of DMF (a few drops) was added to convert the acid into an acid chloride. The reaction mixture was stirred at rt for 2 hours. Then the solvent was removed and the carboxylic acid chloride was used without further purification. In the meantime, n-BuLi (2.19 mL, 5.49 mmol, 2.5 M in hexane) was added to (*R*)-4-benzyloxazolidin-2-one (0.88 g, 4.99 mmol) in 25 mL THF at -78 °C and the reaction mixture was stirred at that temperature for 1 h. Then the acid chloride, dissolved in 5 mL DCM, was added to the deprotonated auxiliary and the mixture was allowed to warm to rt. The reaction was quenched by the addition of 15 mL saturated NH_4Cl and the product was extracted three times with 40 mL Et_2O. The combined organics were then dried over $MgSO_4$, filtered and the solvent was removed under reduced pressure. The product was obtained after purification by flash chromatography (0-10 % EtOAc in cyclohexane) as a yellow oil (1.21 g, 3.55 mmol, 71.1 %). ^1H NMR (599 MHz, $CDCl_3$) δ 7.34 – 7.30 (m, 2H), 7.26 – 7.16 (m, 5H), 6.30 (dtd, *J* = 17.1, 10.3, 0.8 Hz, 1H), 6.15 – 5.98 (m, 1H), 5.68 (dtd, *J* = 15.0, 7.0, 0.8 Hz, 1H), 5.15 – 5.03 (m, 1H), 5.02 – 4.88 (m, 1H), 4.82 – 4.64 (m, 1H), 4.26 – 4.11 (m, 2H), 3.33 (dd, *J* = 13.4, 3.3 Hz, 1H), 2.78 (dd, *J* = 13.4, 9.6 Hz, 1H), 2.30 (qd, *J* = 6.9, 1.2 Hz, 2H), 2.10 (qd, *J* = 7.2, 1.4 Hz, 2H), 1.55 – 1.49 (m, 2H), 1.48 – 1.43 (m, 2H). ^{13}C NMR (101 MHz, $CDCl_3$) δ 165.06, 153.42, 151.64, 137.17, 135.37, 134.80, 131.24, 129.44, 128.93, 127.29, 120.45, 114.92, 66.10, 55.32, 37.89, 32.53, 32.24, 28.67, 27.59, 26.90. MS (ESI^+), calc. 340.19 $[C_{21}H_{25}NO_3+H]^+$, found 340.28 $[M+H]^+$.

(*R*)-4-benzyl-3-((1*R*,4a*S*,8a*R*)-1,2,4a,5,6,7,8,8a-octahydronaphthalene-1-carbonyl)oxazolidin-2-one (11b). The acylated Evans auxiliary **10b** (140 mg, 0.41 mmol) was dissolved in 16.5 mL DCM and cooled to -78 °C. DMAC (0.62 mL, 0.62 mmol, 1 M in hexane) was added and the reaction mixture was stirred for 16 h, whereby it slowly warmed to rt. Then the mixture was quenched with 1 N HCl and the product extracted with DCM. The combined organics were then dried over $MgSO_4$, filtered and the solvent was removed under reduced pressure. The product was obtained after purification by flash chromatography (0-10 % EtOAc in cyclohexane) as a colorless oil (115 mg, 0.34 mmol, 82.1 %). ^{1}H NMR (599 MHz, $CDCl_3$) δ 7.35 – 7.30 (m, 2H), 7.28 – 7.25 (m, 1H), 7.22 – 7.18 (m, 2H), 5.64 – 5.60 (m, 1H), 5.49 – 5.41 (m, 1H), 4.72 – 4.67 (m, 1H), 4.21 – 4.14 (m, 2H), 3.87 (td, *J* = 10.8, 5.7 Hz, 1H), 3.25 (dd, *J* = 13.4, 3.3 Hz, 1H), 2.77 (dd, *J* = 13.4, 9.5 Hz, 1H), 2.41 – 2.35 (m, 1H), 2.32 – 2.24 (m, 1H), 1.88 – 1.81 (m, 1H), 1.79 – 1.68 (m, 3H), 1.69 – 1.62 (m, 1H), 1.61 – 1.49 (m, 1H), 1.34 – 1.28 (m, 2H), 1.12 – 0.99 (m, 2H). ^{13}C NMR (151 MHz, $CDCl_3$) δ 176.37, 153.12, 135.24, 132.09, 129.41, 128.90, 127.32, 123.96, 65.96, 55.29, 43.13, 42.46, 41.09, 37.96, 32.99, 29.95, 29.83, 26.62, 26.44. MS (ESI^+), calc. 340.19 $[C_{21}H_{25}NO_3+H]^+$, found 340.11 $[M+H]^+$.

(1*R*,4a*S*,8a*R*)-1,2,4a,5,6,7,8,8a-octahydronaphthalene-1-carboxylic acid (12b). To cleave the Evans auxiliary **11b** (43 mg, 0.13 mmol) was dissolved in 2 mL THF/H_2O (8:5) followed by the addition of LiOH (14 mg, 0.59 mmol) and H_2O_2 (66 µL, 0.65 mmol, 30 wt.-% in H_2O). The reaction mixture was stirred at rt for 2.5 h and then quenched by adding a half-saturated Na_2SO_3 solution. It was extracted with DCM and the organic layers were removed. Then the aqueous layer

was acidified with concentrated HCl and the product was extracted with DCM. The combined organic layers were dried over $MgSO_4$, filtered and the solvent was removed under reduced pressure to obtain the title compound without further purification as a colorless solid (19 mg, 0.11 mmol, 83.2 %). ^{1}H NMR (300 MHz, $CDCl_3$) δ 5.65 – 5.57 (m, 1H), 5.45 (dq, *J* = 9.9, 1.9 Hz, 1H), 2.48 – 2.39 (m, 1H), 2.38 – 2.29 (m, 2H), 1.87 – 1.71 (m, 4H), 1.68 – 1.21 (m, 4H), 1.19 – 0.99 (m, 2H). ^{13}C NMR (75 MHz, $CDCl_3$) δ 181.95, 132.09, 123.79, 46.17, 42.12, 41.33, 32.94, 30.31, 29.47, 26.58, 26.36.

(3a*R*,5*R*,5a*R*,9a*R*,9b*S*)-2,2-dimethyldecahydronaphtho[1,2-d][1,3]dioxole-5-carboxylic acid (**12d**). **11b** (80 mg, 0.26 mmol) was dissolved in 1.0 mL acetone and 0.5 mL H_2O. Then 4-methylmorpholine-4-oxide (55 mg, 0.47 mmol) and osmium tetroxide (118 µL, 9.4 µmol, 2.5 wt.-% in tBuOH) were added and the mixture was stirred at rt for 16 h. The crude product was directly loaded on silica and purified by flash chromatography (0-50 % [EtOAc + 2 % MeOH] in cyclohexane) to obtain the intermediate as a diastereomeric mixture (dr = 4:1, quant. yield). The intermediate was then dissolved in 1.4 mL acetone and 2,2-dimethoxypropane (1:1) and PTSA (0.02 eq) was added. The reaction was stirred for 24 h and then purified by flash chromatography (0-5 % EtOAc in cyclohexane), whereby the minor diasteroemer was separated, to obtain the protected diol. Then general procedure F (Supporting Information) was used to obtain **12d** without further purification as colorless oil (24 mg, 9.4 µmol, 36.3 % from **11b**). ^{1}H NMR (400 MHz, $CDCl_3$) δ 4.28 – 4.20 (m, 1H), 3.60 (dd, *J* = 8.6, 4.9 Hz, 1H), 2.46 – 2.36 (m, 1H), 2.32 (ddd, *J* = 14.9, 4.0, 2.6 Hz, 1H), 2.13 – 2.04 (m, 1H), 1.96 (ddd, *J* = 14.8, 12.1, 4.0 Hz, 1H), 1.84 – 1.64 (m, 3H), 1.48 (s, 3H), 1.34 (s, 3H), 1.26 – 1.14 (m, 4H), 1.02 (dt, *J* = 10.9, 6.1 Hz, 1H), 0.97 – 0.87 (m, 1H). ^{13}C NMR (101 MHz, $CDCl_3$) δ 181.15, 108.31, 79.53, 72.31, 44.28, 43.73, 40.16, 30.73,

30.12, 29.67, 28.53, 26.38, 25.77, 25.59. MS (ESI$^+$), calculated 255.16 [$C_{14}H_{22}O_4$+H]$^+$, found 255.02 [M+H]$^+$.

(*S*)-(*R*)-3-(3,4-dimethoxyphenyl)-1-(3-(2-morpholinoethoxy)phenyl)propyl 1-((1*S*,4a*S*,8a*R*)-1,2,4a,5,6,7,8,8a-octahydronaphthalene-1-carbonyl)piperidine-2-carboxylate (16). 12b (40.0 mg, 0.22 mmol), **31** (125 mg, 0.24 mmol), HATU (127 mg, 0.33 mmol) and DIPEA (86.0 mg, 0.67 mmol) were stirred in 4 mL DMF at rt for 16 h. The reaction mixture was loaded on silica and purified by flash chromatography (0-100 % [EtOAc + 2 % MeOH + 0.1 % TEA] in cyclohexane) to obtain the title compound as light yellow oil (quantitative yield). ^{1}H NMR (599 MHz, DMSO-d_6) δ 7.26 – 7.21 (m, 1H), 6.88 – 6.80 (m, 4H), 6.75 – 6.70 (m, 1H), 6.67 – 6.62 (m, 1H), 5.59 (dd, J = 8.8, 4.7 Hz, 1H), 5.56 – 5.50 (m, 2H), 5.41 – 5.33 (m, 2H), 5.27 – 5.23 (m, 1H), 3.71 – 3.66 (m, 6H), 3.59 – 3.52 (m, 4H), 2.53 – 2.48 (m, 2H), 2.44 – 2.38 (m, 3H), 2.20 – 2.14 (m, 2H), 2.11 – 2.05 (m, 3H), 1.83 – 1.76 (m, 1H), 1.72 – 1.56 (m, 7H), 1.54 – 1.48 (m, 3H), 1.36 – 1.20 (m, 5H), 1.06 – 1.01 (m, 2H), 0.98 – 0.93 (m, 2H), 0.91 – 0.85 (m, 1H). ^{13}C NMR (151 MHz, $CDCl_3$) δ 179.56, 177.17, 175.45, 167.31, 163.49, 153.81, 152.20, 147.22, 138.31, 136.98, 134.77, 129.69, 125.10, 123.27, 118.96, 117.35, 116.96, 80.59, 71.20, 70.25, 64.78, 62.12, 60.68, 60.40, 58.75, 56.65, 48.13, 47.26, 45.54, 42.66, 40.94, 37.71, 35.78, 34.45, 31.29, 30.14, 26.21, 19.23. HRMS, calc. 675.4009 [$C_{40}H_{54}N_2O_7$+H]$^+$, found 675.3999 [M+H]$^+$. HPLC [0-100% Solvent B, 20 min]: Rt = 13.60 min, 100 %.

(S)-(R)-3-(3,4-dimethoxyphenyl)-1-(3-(2-morpholinoethoxy)phenyl)propyl 1-((1R,4aS,8aR)-3-oxodecahydronaphthalene-1-carbonyl)piperidine-2-carboxylate (24) and (*S*)-(*R*)-3-(3,4-

dimethoxyphenyl)-1-(3-(2-morpholinoethoxy)phenyl)propyl 1-((1*R*,4a*R*,8a*R*)-4-oxodecahydronaphthalene-1-carbonyl)piperidine-2-carboxylate (25). A solution of tetrafluoroboric acid (16 µL, 0.10 mmol, 48 wt.-% in H_2O) and **16** were added to a solution of palladium(II) acetate (0.83 mg, 3.70 µmol) and p-benzoquinone (8.01 mg, 74 µmol) in 0.45 mL MeCN and 0.6 mL H_2O. The reaction mixture was stirred at rt for 16 h and then directly loaded on silica for purificaion by flash chromatography (0-50 % [EtOAc + 2 % MeOH + 0.1 % TEA] in hexane), whereby both products can easily be separated, to obtain title compounds **24** (11.4 mg, 20.9 µmol, 14.8 %, analytics shown in Supplementary Information) and **25** (19.0 mg, 51.1 µmol, 24.7 %) as colorless oils. (25): ^{1}H NMR (599 MHz, $CDCl_3$) δ 7.24 – 7.21 (m, 1H), 6.95 – 6.74 (m, 4H), 6.68 – 6.62 (m, 2H), 5.74 – 5.68 (m, 1H), 5.48 (d, *J* = 4.9 Hz, 1H), 4.15 – 4.04 (m, 2H), 3.97 (d, *J* = 13.5 Hz, 1H), 3.89 – 3.79 (m, 6H), 3.79 – 3.67 (m, 4H), 3.21 (td, *J* = 13.1, 2.8 Hz, 1H), 2.85 (dt, *J* = 11.9, 5.3 Hz, 1H), 2.82 – 2.75 (m, 2H), 2.65 – 2.52 (m, 5H), 2.52 – 2.45 (m, 1H), 2.42 – 2.33 (m, 3H), 2.24 – 2.16 (m, 1H), 2.13 – 1.59 (m, 11H), 1.51 – 1.42 (m, 1H), 1.41 – 1.32 (m, 1H), 1.32 – 1.09 (m, 4H), 0.99 (qd, *J* = 12.3, 3.6 Hz, 1H). (25): ^{13}C NMR (151 MHz, $CDCl_3$) δ 210.44, 173.52, 170.47, 158.80, 148.84, 147.32, 141.40, 133.40, 129.60, 120.10, 118.92, 113.84, 113.20, 111.66, 111.27, 76.24, 66.87, 57.64, 55.90, 55.82, 54.08, 53.16, 52.06, 45.67, 44.50, 43.51, 40.36, 37.93, 32.29, 31.22, 29.40, 26.82, 25.61, 25.42, 25.30, 25.14, 21.11. HRMS, calc. 691.3958 $[C_{40}H_{54}N_2O_8+H]^+$, found 691.3991 [M(**25**)+H]$^+$. HPLC [0-100% Solvent B, 20 min]: Rt = 15.48 min, 99 %.

(2*S*)-(*R*)-3-(3,4-dimethoxyphenyl)-1-(3-(2-morpholinoethoxy)phenyl)propyl-1-((5*R*,5a*R*,9a*R*)-2,2-dimethyldecahydronaphtho[1,2-d][1,3]dioxole-5-carbonyl)piperidine-2-carboxylate (28). 12d (20.0 mg, 0.08 mmol), **31** (44.3 mg, 0.09 mmol), HATU (44.9 mg, 0.12

mmol) and DIPEA (30.5 mg, 0.236 mmol) were stirred in 2 mL DMF at rt for 18 h. The orange reaction mixture was loaded on silica and purified by flash chromatography (0-100 % [EtOAc + 2 % MeOH + 0.1 % TEA] in cyclohexane) to obtain the title compound as light yellow oil (45.5 mg, 0.06 mmol, 77.2 %). ^{1}H NMR (599 MHz, DMSO-d_6) δ 7.28 – 7.20 (m, 1H), 6.88 – 6.79 (m, 4H), 6.75 – 6.71 (m, 1H), 6.67 – 6.60 (m, 1H), 5.58 (dd, J = 8.8, 4.7 Hz, 1H), 5.21 (d, J = 6.0 Hz, 0H), 4.20 (d, J = 6.7 Hz, 1H), 4.14 – 4.02 (m, 3H), 3.93 (d, J = 13.4 Hz, 1H), 3.72 – 3.64 (m, 6H), 3.60 – 3.52 (m, 4H), 3.09 – 2.99 (m, 1H), 2.98 – 2.91 (m, 1H), 2.87 – 2.75 (m, 0H), 2.71 – 2.66 (m, 2H), 2.43 (ddd, J = 13.7, 8.3, 4.6 Hz, 1H), 2.19 – 2.12 (m, 2H), 2.09 – 2.01 (m, 2H), 1.98 – 1.95 (m, 2H), 1.77 – 1.48 (m, 8H), 1.44 – 1.31 (m, 5H), 1.29 – 1.04 (m, 8H), 1.02 – 0.66 (m, 4H), 0.30 – 0.20 (m, 1H). ^{13}C NMR (151 MHz, DMSO-d_6) δ 174.96, 170.87, 158.85, 149.02, 147.46, 142.43, 133.64, 130.04, 120.38, 120.33, 118.68, 114.34, 112.59, 112.32, 75.86, 74.86, 68.72, 66.47, 65.58, 57.36, 55.93, 55.78, 53.98, 51.88 38.45, 38.06, 34.59, 31.05, 30.85, 29.45, 29.37, 26.90, 26.77, 26.26, 26.13, 25.39, 22.53, 21.18. HRMS, calc. 749.4377 $[C_{43}H_{60}N_2O_9+H]^+$, found 749.4380 $[M+H]^+$. HPLC [0-100% Solvent B, 20 min]: Rt = 16.87 min, 97 %.

(*S*)-(*R*)-3-(3,4-dimethoxyphenyl)-1-(3-(2-morpholinoethoxy)phenyl)propyl 1-((1*R*,3*R*,4*S*,4a*R*,8a*R*)-3,4-dihydroxydecahydronaphthalene-1-carbonyl)piperidine-2-carboxylate (29). 28 (40 mg, 53 µmol) was stirred in 1.86 mL MeOH and concentrated 0.14 mL HCl for 1.5 h at rt. Then the solvent was removed under reduced pressure. Compound **29** (11.5 mg, 16.2 µmol, 30.3 %) was obtained after purification by preparative HPLC (40-50 % solvent B). ^{1}H NMR (599 MHz, DMSO-d_6) δ 7.26 – 7.22 (m, 1H), 6.88 – 6.83 (m, 3H), 6.82 – 6.79 (m, 1H), 6.74 – 6.71 (m, 1H), 6.66 – 6.62 (m, 1H), 5.58 (dd, J = 8.8, 4.7 Hz, 1H), 5.23 (d, J = 6.1 Hz, 1H), 4.11 – 4.00 (m, 3H), 3.95 (d, J = 13.2 Hz, 1H), 3.69 (d, J = 11.7 Hz, 6H), 3.57 – 3.52 (m, 4H),

3.49 (td, J = 8.8, 4.8 Hz, 1H), 3.06 (td, J = 13.1, 2.9 Hz, 1H), 2.76 – 2.69 (m, 1H), 2.65 (q, J = 7.6, 6.5 Hz, 2H), 2.43 (tt, J = 9.2, 4.3 Hz, 4H), 2.18 – 2.12 (m, 1H), 2.11 – 2.05 (m, 1H), 2.02 – 1.93 (m, 2H), 1.92 – 1.86 (m, 1H), 1.76 – 1.69 (m, 1H), 1.68 – 1.60 (m, 3H), 1.59 – 1.46 (m, 3H), 1.36 – 1.28 (m, 2H), 1.24 – 1.16 (m, 3H), 1.14 – 1.03 (m, 3H), 0.88 – 0.76 (m, 2H). ^{13}C NMR (151 MHz, DMSO-d_6) δ 174.49, 170.79, 158.87, 149.04, 147.49, 142.36, 133.60, 130.00, 120.38, 118.76, 114.33, 112.57, 112.31, 107.78, 79.10, 75.90, 72.55, 66.60, 57.42, 55.92, 55.78, 54.05, 52.01, 43.48, 43.35, 37.91, 31.03, 30.34, 30.19, 29.60, 29.05, 26.87, 25.96, 25.85, 25.38, 21.06. HRMS, calc. 709.4064 $[C_{40}H_{56}N_2O_9+H]^+$, found 709.4089 $[M+H]^+$. HPLC [0-100% Solvent B, 20 min]: Rt = 14.28 min, 96 %.

Analysis of apoptosis

Analysis of DNA content by propidium iodide incorporation was performed in permeabilized cells by flow cytometry. Cells (1×10^5) were harvested following incubation with the drug, washed in PBS and resuspended in 500 µL of a solution containing 0.1% sodium citrate w/v, 0.1% Triton X-100 v/v and 50 µg/mL propidium iodide (Sigma Chemical Co, Gallarate, Italy). Following incubation at 4°C for 30 min in the dark, cell nuclei were analyzed with a Becton Dickinson FACScan flow-cytometer. Cellular debris were excluded from analysis by raising the forward scatter threshold and the DNA content of the nuclei was registered on a logarithmic scale. The percentage of the elements in the hypodiploid region was calculated.

Apoptosis was measured using propidium iodide in double staining with annexin V-FITC (BD Biosciences, NJ, USA). Annexin V binds to phosphatidylserine, which, in dying cells, is exposed on the outer leaflet of plasma membrane. Propidium iodide does not stain cells with intact membrane, as it occurs in early apoptosis. Briefly, 1×10^5 cells were resuspended in 100 µL of binding buffer (10 mM Hepes/NaOH pH 7.5, 140 mM NaCl, 2.5 mM $CaCl_2$) containing 5 µL of

annexin V-FITC (Pharmingen/Becton Dickinson, San Diego, CA, USA) and 10 µl of PI solution without Triton. Cells were incubated for 15 min at room temperature in the dark and analyzed with C6 BDAccuri flow cytometer (Becton Dickinson).

Statistical analysis

Student's t-test was used to assess differences between means of values. A p-value of ≤ 0.05 was considered significant.

ANCILLIARY INFORMATION

Supporting Information

Further experimental details (Suppl. Fig. 1 - 6; Suppl. Tab. 1 & 2, crystallograhic data collection and refinement statistics, NMR spectra, biological, biochemical and synthetic procedures of all remaining compounds, list of SI items incl. Molecular Formula Strings) are provided in the Supporting Information which is available free of charge on the ACS Publications website at DOI: XXX

Accession Codes

Atomic coordinates for the X-ray structure of compound **25** in complex with FKBP51 (16-140)-A19T (PDB code 6SAF) are available from the RCSB Protein Data Bank (www. rcsb.org). Authors will release the atomic coordinates and experimental data upon article publication.

AUTHOR INFORMATION

Corresponding Author

*Email: hausch@drugdiscovery.chemie.tu-darmstadt.de

ORCID

Felix Hausch: 0000-0002-3710-8838

Present Address

Technical University Darmstadt, Alarich-Weiss-Str. 4, 64287 Darmstadt, Germany.

ACKNOWLEDGEMENTS

This work was supported by the M4 Awards 2011 and 2015 from the StMWIVT (3662a/89/6 and BIO-1601-0003 to FH) and by the Pioneer Fund (ENTEGA/TU Darmstadt to FH). We are indebted to Mrs. E. Weyher and Dr. S. Uebel (MPI of Biochemistry) for the HRMS measurement and to Mrs. C. Dubler and Dr. D. Stephenson (Ludwig-Maximilians University of Munich) for NMR measurements and the JSBG staff at the European Synchrotron Radiation Facility (ESRF) in Grenoble, France.

ABBREVIATIONS USED

COMU (1-Cyano-2-ethoxy-2-oxoethylidenaminooxy)dimethylamino-morpholino-carbenium hexafluorophosphate, DCC N,N'-Dicyclohexylcarbodiimide, DIPEA N,N-Diisopropylethylamine, DMAC dimethylaluminium chloride, DMAP 4-(Dimethylamino)pyridine, MS (ESI^+) electrospray ionization mass spectrometry, FKBP FK506-binding protein, HATU 1-[Bis(dimethylamino)methylene]-1H-1,2,3-triazolo[4,5-b]pyridinium 3-oxid hexafluorophosphate, HRMS high-resolution mass spectrometry , nBuLi n-Butyllithium, NMO 4-methylmorpholine 4-oxide, pTsOH p-Toluenesulfonic acid, pyBrop Bromotripyrrolidinophosphonium hexafluorophosphate

REFERENCES

1. Hahle, A.; Merz, S.; Meyners, C.; Hausch, F. The many faces of FKBP51. *Biomolecules* **2019**, 9, 35.
2. Schmidt, M.V.; Paez-Pereda, M.; Holsboer, F.; Hausch, F. The prospect of FKBP51 as a drug target. ChemMedChem **2012**, 7, 1351-1359.
3. Riggs, D.L.; Roberts, P.J.; Chirillo, S.C.; Cheung-Flynn, J.; Prapapanich, V.; Ratajczak, T.; Gaber, R.; Picard, D.; Smith, D.F. The Hsp90-binding peptidylprolyl isomerase FKBP52 potentiates glucocorticoid signaling in vivo. *EMBO J.* **2003** 22, 1158-1167.
4. Romano, S.; Xiao, Y.; Nakaya, M; D'Angelillo, A; Chang, M.; Jin, J.; Hausch, F.; Masullo, M.; Feng, X.; Romano, M.F.; Sun, S.C. FKBP51 employs both scaffold and isomerase functions to promote NF-κB activation in melanoma. *Nucleic Acids Res.* **2015**, 43, 6983-6993
5. Matosin, N.; Halldorsdottir, T.; Binder, E.B. Understanding the molecular mechanisms underpinning gene by environment interactions in psychiatric disorders: The FKBP5 model. *Biol. Psychiatry* **2018**, 83, 821-830.
6. Hernández-Díaz, Y.; González-Castro, T.B.; Tovilla-Zárate, C.A.; Juárez-Rojop, I.E.; López-Narváez, M.L.; Pérez-Hernández, N.; Rodríguez-Pérez, J.M.; Genis-Mendoza, A.D. Association between FKBP5 polymorphisms and depressive disorders or suicidal behavior: A systematic review and meta-analysis study. *Psychiatry Res.* **2019**, 271, 658-668.
7. Touma, C.; Gassen, N.C.; Herrmann, L.; Cheung-Flynn, J.; Büll, D.R.; Ionescu, I.A.; Heinzmann, J.M.; Knapman, A.; Siebertz, A.; Depping, A.M.; Hartmann, J.; Hausch, F.; Schmidt, M.V.; Holsboer, F.; Ising, M.; Cox, M.B.; Schmidt, U.; Rein, T. FK506 Binding Protein 5 Shapes Stress responsiveness: Modulation of neuroendocrine reactivity and coping behavior. *Biol. Psychiatry* **2011**, 70, 928-936.
8. O'Leary, J.C. 3rd; Dharia, S.; Blair, L.J.; Brady, S.; Johnson, A.G.; Peters, M.; Cheung-Flynn, J.; Cox, M.B.; de Erausquin, G.; Weeber, E.J.; Jinwal, U.K.; Dickey, C.A. A new anti-depressive strategy for the elderly: ablation of FKBP5/FKBP51. *PLoS One* **2011**, 6, e24840.
9. Hartmann, J.; Wagner, K.V.; Liebl, C.; Scharf, S.H.; Wang, X.D.; Wolf, M.; Hausch, F.; Rein, T.; Schmidt, U.; Touma, C.; Cheung-Flynn, J.; Cox, M.B.; Smith, D.F.; Holsboer, F.; Muller, M.B.; Schmidt, M.V. The involvement of FK506-binding protein 51 (FKBP5) in the behavioral and neuroendocrine effects of chronic social defeat stress. *Neuropharmacology* **2012**, 62, 332-339.
10. Albu, S.; Romanowski, C. P.; Letizia Curzi, M.; Jakubcakova, V.; Flachskamm, C.; Gassen, N. C.; Hartmann, J.; Schmidt, M. V.; Schmidt, U.; Rein, T.; Holsboer, F.; Hausch, F.; Paez-Pereda, M.; Kimura, M. Deficiency of FK506-binding protein (FKBP) 51 alters sleep architecture and recovery sleep responses to stress in mice. *J. Sleep Res.* **2014**, 23, 176-185.
11. Balsevich, G.; Hausl, A. S.; Meyer, C. W.; Karamihalev, S.; Feng, X.; Pohlmann, M. L.; Dournes, C.; Uribe-Marino, A.; Santarelli, S.; Labermaier, C.; Hafner, K.; Mao, T.; Breitsamer, M.; Theodoropoulou, M.; Namendorf, C.; Uhr, M.; Paez-Pereda, M.; Winter, G.; Hausch, F.; Chen, A.; Tschop, M. H.; Rein, T.; Gassen, N. C.; Schmidt, M. V. Stress-responsive FKBP51 regulates AKT2-AS160 signaling and metabolic function. *Nat. Commun.* **2017**, 8, 1725.
12. Stechschulte, L.A.; Qiu, B.; Warrier, M.; Hinds, T.D. Jr; Zhang, M.; Gu, H.; Xu, Y.; Khuder, S.S.; Russo, L.; Najjar, S.M.; Lecka-Czernik, B.; Yong, W.; Sanchez, E.R. FKBP51 Null mice are resistant to diet-induced obesity and the PPARγ agonist rosiglitazone. *Endocrinology* **2016**, 157, 3888-3900.
13. Maiaru, M.; Morgan, O. B.; Mao, T.; Breitsamer, M.; Bamber, H.; Pohlmann, M.; Schmidt, M. V.; Winter, G.; Hausch, F.; Geranton, S. M. The stress regulator FKBP51: a novel

and promising druggable target for the treatment of persistent pain states across sexes. *Pain* **2018**, 159, 1224-1234.
14. Maiaru, M.; Tochiki, K. K.; Cox, M. B.; Annan, L. V.; Bell, C. G.; Feng, X.; Hausch, F.; Geranton, S. M. The stress regulator FKBP51 drives chronic pain by modulating spinal glucocorticoid signaling. *Sci. Transl. Med.* **2016**, 8, 325ra19.
15. D'Arrigo, P.; Digregorio, M.; Romano, S.; Tufano, M.; Rea, A.; Hausch, F.; Dedobbeleer, M.; Vigorito, V.; Russo, S.; Rogister, B.; Romano, M.F. The splicing FK506 binding protein-51 isoform plays a role in human glioblastoma resistance through Programmed Cell Death Ligand-1 expression regulation. *Cell Death. Discov.* **2019**, 5, 137.
16. Feng, X.; Pomplun, S.; Hausch, F. Recent progress in FKBP ligand development. *Curr. Mol. Pharmacol.* **2015**, 9, 27-36.
17. Dunyak, B. M.; Gestwicki, J. E. Peptidyl-proline isomerases (PPIases): Targets for natural products and natural product-inspired compounds. *J. Med. Chem.* **2016**, 59, 9622-9644.
18. Kolos, J. M.; Voll, A. M.; Bauder, M.; Hausch, F. FKBP ligands-where we are and where to go? *Front. Pharmacol.* **2018**, 9, 1425.
19. Gopalakrishnan, R.; Kozany, C.; Wang, Y.; Schneider, S.; Hoogeland, B.; Bracher, A.; Hausch, F. Exploration of pipecolate sulfonamides as binders of the FK506-binding proteins 51 and 52. *J. Med. Chem.* **2012**, 55, 4123-4131.
20. Gopalakrishnan, R.; Kozany, C.; Gaali, S.; Kress, C.; Hoogeland, B.; Bracher, A.; Hausch, F. Evaluation of synthetic FK506 analogues as ligands for the FK506-binding proteins 51 and 52. *J. Med. Chem.* **2012**, 55, 4114-4122.
21. Wang, Y.; Kirschner, A.; Fabian, A. K.; Gopalakrishnan, R.; Kress, C.; Hoogeland, B.; Koch, U.; Kozany, C.; Bracher, A.; Hausch, F. Increasing the efficiency of ligands for FK506-binding protein 51 by conformational control. *J. Med. Chem.* **2013**, 56, 3922-3935.
22. Bischoff, M.; Sippel, C.; Bracher, A.; Hausch, F. Stereoselective construction of the 5-hydroxy diazabicyclo[4.3.1]decane-2-one scaffold, a privileged motif for FK506-binding proteins. *Org. Lett.* **2014**, 16, 5254-5257.
23. Pomplun, S.; Wang, Y.; Kirschner, A.; Kozany, C.; Bracher, A.; Hausch, F. Rational design and asymmetric synthesis of potent and neurotrophic ligands for FK506-binding proteins (FKBPs). *Angew. Chem. Int. Ed. Engl.* **2015**, 54, 345-348.
24. Pomplun, S.; Sippel, C.; Hahle, A.; Tay, D.; Shima, K.; Klages, A.; Unal, C. M.; Riess, B.; Toh, H. T.; Hansen, G.; Yoon, H. S.; Bracher, A.; Preiser, P.; Rupp, J.; Steinert, M.; Hausch, F. Chemogenomic profiling of human and microbial FK506-binding proteins. *J. Med. Chem.* **2018**, 61, 3660-3673.
25. Hausch, F. FKBPs and their role in neuronal signaling. *Biochimica et Biophysica Acta (BBA) - General Subjects* **2015**, 1850, 2035-2040.
26. Cheung-Flynn, J.; Prapapanich, V.; Cox ,M.B.; Riggs, D.L.; Suarez-Quian, C.; Smith, D.F. Physiological role for the cochaperone FKBP52 in androgen receptor signaling. *Mol. Endocrinol.* **2005**, 19, 1654-1666.
27. Yang, Z.; Wolf, I.M.; Chen H.; Periyasam, S.; Chen, Z.; Yong, W.; Shi, S.; Zhao, W.; Xu, J.; Srivastava, A.; Sánchez, E.R.; Shou, W. FK506-binding protein 52 is essential to uterine reproductive physiology controlled by the progesterone receptor A isoform. *Mol. Endocrinol.* **2006**, 20, :2682-2694.
28. Jagtap, P. K. A.; Asami, S.; Sippel, C.; Kaila, V. R. I.; Hausch, F.; Sattler, M. Selective inhibitors of FKBP51 employ conformational selection of dynamic invisible states. *Angew. Chem. Int. Ed. Engl.* **2019**, 58, 9429–9433.

29. Gaali, S.; Kirschner, A.; Cuboni, S.; Hartmann, J.; Kozany, C.; Balsevich, G.; Namendorf, C.; Fernandez-Vizarra, P.; Sippel, C.; Zannas, A. S.; Draenert, R.; Binder, E. B.; Almeida, O. F.; Ruhter, G.; Uhr, M.; Schmidt, M. V.; Touma, C.; Bracher, A.; Hausch, F. Selective inhibitors of the FK506-binding protein 51 by induced fit. *Nat. Chem. Biol.* **2015**, 11, 33-37.
30. Feng, X.; Sippel, C.; Bracher, A.; Hausch, F. Structure-affinity relationship analysis of selective FKBP51 ligands. *J. Med. Chem.* **2015**, 58, 7796-7806.
31. Gaali, S.; Feng, X.; Hahle, A.; Sippel, C.; Bracher, A.; Hausch, F. Rapid, structure-based exploration of pipecolic acid amides as novel selective antagonists of the FK506-binding protein 51. *J. Med. Chem.* **2016**, 59, 2410-2422.
35. Note that a direct connection of the ortho positions of the trimethoxyphenyl and cyclohexyl rings would require a rotation of the trimethoxyphenyl ring by 90 degrees, which is predicted to disrupt key interaction and impose substantial clashes with the protein.
36. Kozany, C.; Marz, A.; Kress, C.; Hausch, F. Fluorescent probes to characterise FK506-binding proteins. *Chembiochem* **2009**, 10, 1402-1410.
37. Evans, D. A.; Chapman, K. T.; Bisaha, J. Asymmetric Diels-Alder cycloaddition reactions with chiral .alpha.,.beta.-unsaturated N-acyloxazolidinones. *Journal of the American Chemical Society* **1988**, 110, 1238-1256.
38. Biannic, B.; Aponick, A. Gold-catalyzed dehydrative transformations of unsaturated alcohols. *European Journal of Organic Chemistry* **2011**, 2011, 6605-6617.
39. van der Knaap, M.; Basalan, F.; van de Mei, H. C.; Busscher, H. J.; van der Marel, G. A.; Overkleeft, H. S.; Overhand, M. Synthesis and biological evaluation of gramicidin S-inspired cyclic mixed α/β-peptides. *Chemistry & Biodiversity* **2012**, 9, 2494-2506.
40. Morandi, B.; Wickens, Z. K.; Grubbs, R. H. Regioselective wacker oxidation of internal alkenes: Rapid access to functionalized ketones facilitated by cross-metathesis. *Angewandte Chemie International Edition* **2013**, 52, 9751-9754.
41. Laube, T.; Beil, W.; Seifert, K. Total synthesis of two 12-nordrimanes and the pharmacological active sesquiterpene hydroquinone yahazunol. *Tetrahedron* **2005**, 61, 1141-1148.
42. A structure-activity relationship analysis across of closely related analogs between the SAFit1 vs SAFit2 class (e.g. 20/24, 20/25, 21/26) seems to be valid, since all direct analogs between the SAFit1 vs SAFit2 class (e.g. SAFit1 vs SAFit2, 14 vs 16, 17 vs 18) have nearly identical affinities to FKBP51.
43. Bracher, A.; Kozany, C.; Thost, A. K.; Hausch, F. Structural characterization of the PPIase domain of FKBP51, a cochaperone of human Hsp90. *Acta. Crystallogr. D. Biol. Crystallogr.* **2011**, 67, 549-559.

Table of Contents graphic

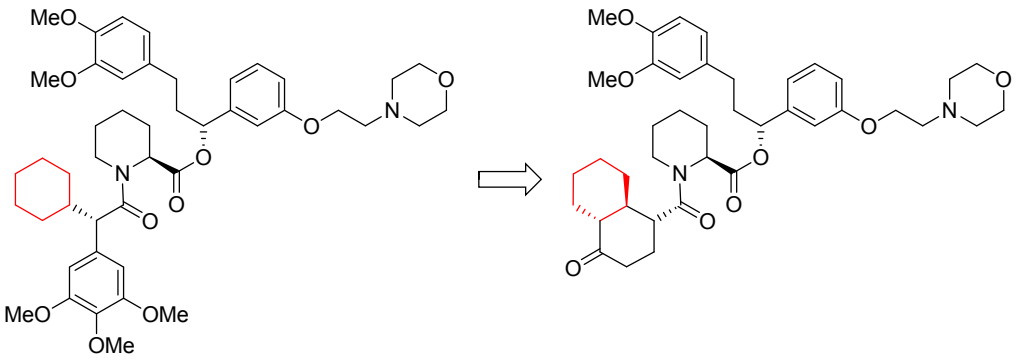

Selectivity towards FKBP51 can be retained by the decalin scaffold